CHEMICAL ENGINEERING TRANSACTIONS
VOL. 56, 2017
A publication of AIDIC
The Italian Association of Chemical Engineering
Online at www.aidic.it/cet
Guest Editors: Jiří Jaromír Klemeš, Peng Yen Liew, Wai Shin Ho, Jeng Shiun Lim

ISBN 978-88-95608-47-1; **ISSN** 2283-9216
DOI: 10.3303/CET1756186

Photocatalytic CO_2 Reduction to CO over Fe-loaded TiO_2/Nanoclay Photocatalyst

Beenish Tahir, Muhammad Tahir*, Nor Aishah Saidina Amin

Chemical Reaction Engineering Group (CREG), Department of Chemical Engineering, Faculty of Chemical and Energy Engineering, Universiti Teknologi Malaysia (UTM), 81310 UTM Johor Bahru, Johor, Malaysia.
mtahir@cheme.utm.my

Fe-promoted titanium dioxide (TiO_2) nanoparticles dispersed in Montmorillonite (MMT) clay for dynamic photocatalytic carbon dioxide (CO_2) reduction to carbon monoxide (CO) and hydrocarbons in a monolith photo-reactor has been investigated. MMT-clay supported Fe/TiO_2 nanocomposites were prepared by a controlled and direct sol-gel method and were dip-coated over the monolith micro-channels. The performance of Fe-loaded MMT/TiO_2 nano-catalyst for CO_2 reduction by H_2 toward CO evolution was evaluated in a continuous operation of photo-reactor under UV-light irradiation. The photo-activity of TiO_2 catalyst dispersed in MMT and loaded with Fe was significantly enhanced. The maximum yield of CO over 3 wt% Fe - 10 wt% MMT-loaded TiO_2 catalyst reached to 289.30 µmole g-cat^{-1} h^{-1} at selectivity 99.61 %, is considerably higher than the amount produced over the MMT/TiO_2 (25.95 µmole g-cat^{-1} h^{-1}) and the pure TiO_2 (8.52 µmole g-cat^{-1} h^{-1}) catalyst. The other products observed with adequate amounts were CH_4 and C_2H_6. These results revealed significantly enhanced photo-activity of TiO_2 loaded with Fe and dispersed over MMT. The enhanced CO evolution was evidently due to larger illuminated active surface area, higher adsorption process inside the monolith micro-channels and hindered charges recombination rate by Fe. This development has confirmed higher photoactivity of Fe-MMT/TiO_2 photo-catalyst for continuous CO_2 photo-reduction to cleaner fuels.

1. Introduction

Greenhouse gas carbon dioxide (CO_2) emitted from the excessive burning of fossil fuels is the primary cause of global warming (Tahir et al., 2015b). CO_2 is very stable and inert molecule while its conversion to fuels using a thermal catalytic process is an energy-consuming process (Yang et al., 2016). Photocatalytic conversion of CO_2 with H_2O to fuels such as CH_3OH (Yu et al., 2015), CH_4 (He et al., 2016) and CO (Tahir et al., 2016a) by the use of light irradiation provides pathways towards economical and sustainable process. However, lower yield rates and selectivity has been reported as H_2O is hardly reducible and CO_2 conversion by H_2O yielded lower amounts of products (Olivo et al., 2015). CO_2 conversion to fuels by hydrogen as a reducing agent has been reported as the most attractive method (Tahir et al., 2015a).
Among the various semiconductor materials, titanium dioxide (TiO_2) has attracted many researchers in recent years due to its numerous advantages such as relatively low price, available in excess, photo-stable, non-toxic and has high oxidative potentials (Paulino et al., 2016). However, TiO_2 photocatalytic efficiency is lower because of fast recombination of photo-generated electron holes pairs. One of the potentials to enhance TiO_2 photocatalytic activity is by its dispersion into the clay micro-sheets. Using nanoclay as a support in which TiO_2 can be distributed on the surface of a suitable matrix, clay-TiO_2 hetero-junction is formed (Kameshima et al., 2009). The additional benefits of using clay as a green materials are their low cost, environment friendly and high CO_2 adsorption capacity (Bhattacharyya et al., 2008).
The most widely used clay minerals for photocatalytic applications is Montmorillonite (MMT). MMT has high sorption capacity in addition of charge trapping ability (Kočí et al., 2014). By dispersing TiO_2 over MMT layers, clay-TiO_2 hetero-junction is produced, resulting in the enhanced TiO_2 photocatalytic activity. Previously, we investigated TiO_2/MMT nanocomposites and observed higher efficiency for photocatalytic CO_2 reduction by H_2O to CH_4 (Tahir et al., 2013). The photocatalytic activity of MMT/TiO_2 photocatalyst can be further enhanced

Please cite this article as: Tahir B., Tahir M., Amin N.A.S., 2017, Photocatalytic co2 reduction to co over fe-loaded tio2/nanoclay photocatalyst, Chemical Engineering Transactions, 56, 1111-1116 DOI:10.3303/CET1756186

by loading suitable metal ions. During the last years, various transition metal ions (Fe, Zn, V) have been selected to incorporate with TiO_2, overcoming the limitation of fast recombination of photo-generated charges (Guo et al., 2016). Fe-ions incorporated into crystal lattice of TiO_2 has been investigated for degradation of pollutants under UV and visible light irradiations. The enhanced photoactivity was evidently due to promoting Fe/TiO_2 interfacial charge transfer process (Harifi et al., 2014). To the best of our knowledge, the application of Fe-promoted TiO_2/MMT nanocomposites for the conversion of CO_2 to CO with H_2 as a reducing agent in a monolith photoreactor has never been reported. Further research involving MMT supported Fe/TiO_2 photocatalyst for gas phase CO_2 conversion in a continuous monolith photoreactor to produce renewable fuels is warranted.

MMT-clay modify TiO_2 structure promoted by Fe has been synthesised by sol-gel method and was immobilised onto monolith microchannels. The performance analysis of the nanocomposites was investigated for selective and dynamic photocatalytic CO_2 reduction with H_2 to CO in a continuous operation of photoreactor. The photocatalytic reaction mechanism for CO_2 reduction to CO were analysed based on the experimental results.

2. Experimental

2.1 Catalyst preparation and Characterisation

Fe-loaded MMT/TiO_2 nanocomposites were synthesised through a single step sol-gel method using Tetra-isopropyl orthotitanate (98 %, Merck), MMT (1.4 P, Sigma-Aldrich) and $FeNO_3$ H_2O (Sigma-Aldrich). 20 mL titanium solution dispersed in 45 mL isopropanol was taken into flask for the hydrolysis process. The solution was hydrolysed by adding 15 mL acetic acid (1 M) diluted in 20 mL isopropanol under vigorous stirring. The mixture was stirred for 12 h to get clear titanium sol. Next, the appropriate amount of $FeNO_3.9H_2O$ dissolved in isopropanol were added to above solution and stirred for another 6 h. Subsequently, MMT dispersed in isopropanol was added into sol and process of gelation was continued by stirring the mixture for another 6 h until the thick sol was obtained. The sol obtained was transferred into a glass container for the monolith coating. Next, the dried monoliths were dipped into the sol. The coating process was repeated to ensure desired amount of catalyst coating. Any excess sol was blown off using hot compressed air. The coated monoliths were dried at 80 °C for 12 h before calcined at 500 °C for 5 h. Catalyst loading was calculated by subtracting coated monolith weight from the initial bare monolith weight.

The catalysts were characterised using powder X-ray diffraction (XRD) and scanning electron microscopy (SEM). The crystalline phase was investigated using powder X-ray diffraction (XRD; Bruker D8 advance diffractometer, 40 kV and 40 mA) with Cu-Kα radiation (λ = 1.54 A°). The scanning electron microscopy (SEM) was carried out with JEO L JSM6390 LV SEM instrument.

2.2 Photoactivity test

The reactor consists of stainless steel cylindrical vessel with a length of 5.5 cm and total volume of 150 cm^3. The catalyst coated monoliths were introduced inside the cylindrical stainless steel chamber, equipped with a quartz window for passing light irradiations using 200 W Hg lamp (Epson elplp 67). An optical process monitor ILT OPM-1D and a SED008/W sensor was placed above the upper surface of the monolith to measure light intensity entering into the channels. Prior to feeding, the reactor chamber was purged using purified helium (He) flow, then a mixture of gases (CO_2, H_2 and He) was constantly streamed through the reactor for 1 h to saturate the catalyst. The products were analysed using an on-line gas chromatograph (GC-Agilent Technologies 6890 N, USA) equipped with thermal conductivity detector (TCD) and flame ionised detector (FID).

3. Results and discussion

3.1 Catalyst characterisation

XRD plots of TiO_2, MMT and Fe-loaded TiO_2 nano-composites are shown in Figure 1. The peaks of TiO_2 calcined at 500 °C revealed a pure anatase and crystalline phase. The XRD pattern of MMT presents a broad basal reflection of (0 0 1) at 2θ = 3.70°, evidently due to the orientation of platy-shaped particles and stacking disorder of MMT layers. In the case of MMT and Fe-loaded TiO_2 samples, TiO_2 persisted its original reflection with no additional peak appeared, however, all TiO_2 peaks become broader and weaker. This was probably due to the fact that MMT hindered TiO_2 crystal growth, resulting in reduced crystallite size (Tahir et al., 2015c). The prominent MMT peak (001) due to the layered clay has also disappeared in all MMT based samples. This revealed that the layered structure of the MMT has disordered with uniform dispersion of TiO_2 NPs. This

resulted in controlled crystal growth of TiO_2 NPs and similar observations has been reported previously (Tahir et al., 2015c).

The morphology of TiO_2 and modified TiO_2 samples is presented in Figure 2. Figure 2 (a) reveals spherical shape and uniform size of TiO_2 nanoparticles. The MMT image in Figure 2 (b) shows stacked MMT layers with disorder structures. Figure 2 (c) illustrates SEM images of TiO_2 dispersion over the MMT layers and Fe-loaded MMT/TiO_2 samples. MMT layers are completely destroyed and TiO_2 NPs are well distributed over the MMT surface and producing MMT/TiO_2 nanocomposite. The morphology of Fe-loaded MMT/TiO_2 sample is much similar to MMT/TiO_2 composite, where MMT layers are destroyed as presented in Figure 2(d). These observations have confirmed well-developed Fe-loaded MMT/TiO_2 nanocomposites.

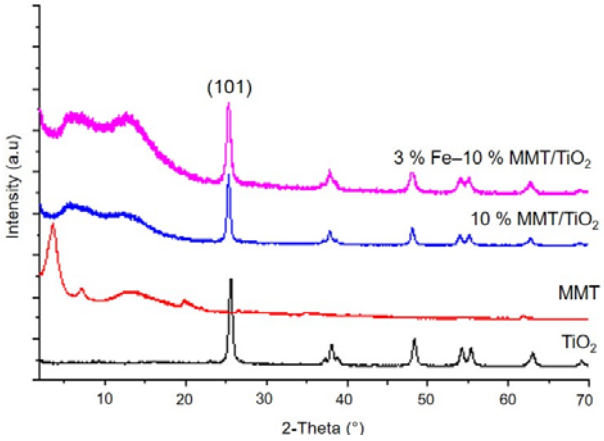

Figure 1: X-ray diffraction patterns of TiO_2, MMT and Fe-MMT/TiO_2 catalysts

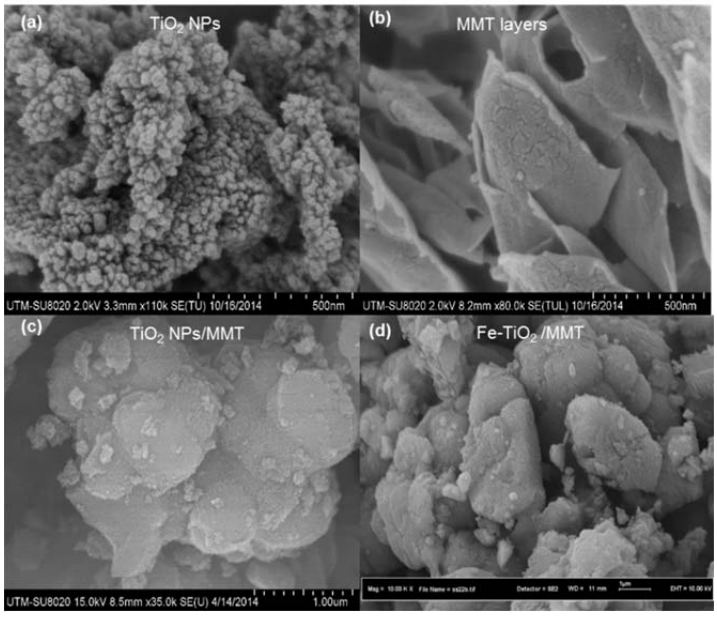

Figure 2: SEM images of TiO_2 and TiO_2/MMTs samples: (a-b) SEM images of MMT layers; (c) SEM image of TiO_2 nanoparticles; (d) SEM image of TiO_2/MMT sample

3.2 Photocatalytic CO_2 reduction with H_2

Control experiments were conducted to confirm all the products were obtained during CO_2 photo-reduction process. Using all types of catalysts, carbon containing compounds were not detected in the reaction system without reactants or light irradiations. Any carbon containing compounds produced were derived from CO_2 photo-reduction with CO found to be a major CO_2 photo-reduction product in all the experiments.

The effects of MMT onto TiO_2 performance for CO_2 photo-reduction with H_2 to CO and CH_4 is presented in Figure 3 (a). CO was detected as the main product over all types of photo-catalysts, which has confirmed favourable reaction using monolith as the photoreactor and hydrogen as a reducing agent. Pure TiO_2 has low photoactivity for CO production, which gradually increased in MMT supported TiO_2 samples. This was evidently due to efficient charge transfer, higher surface area and efficient CO_2 adsorption in MMT/TiO_2 samples. Loading MMT into TiO_2 has significantly improved CO_2 photo-reduction with optimum MMT-loading of 10 wt%. 10 wt% MMT-loaded TiO_2 sample was the most active over which continuous production of CO was the highest. With more MMT loading (e.g., 15 wt%) into TiO_2, photoactivity was gradually reduced. This was certainly reduced in photo-catalyst (TiO_2) active sites and perhaps due to shading effect inside the monolith micro-channels by excessive MMT-loading.

The effect of Fe-loading on the photoactivity of MMT/TiO_2 for selective photocatalytic CO evolution is presented in Figure 3 (b). Much higher CO production was detected over Fe-loaded MMT/TiO_2 compared to MMT/TiO_2 and pure TiO_2 samples over the entire irradiation time. The significantly enhanced photoactivity of Fe-loaded TiO_2 samples were evidently due to efficient charges separation with hindered recombination rate by Fe. Since the continuous flow mode of monolith photoreactor was used, initially the production of CO reached to maximum, then gradually process reduced to steady state after 4 h of irradiation time. The results also confirmed prolonged stability of Fe-promoted MMT/TiO_2 samples for dynamic CO_2-to-CO conversion.

The performance of Fe on the photoactivity of MMT/TiO_2 for photocatalytic CO_2 conversion with H_2 to CH_4 and C_2H_6 is presented in Figure 4. Using pure TiO_2, only small amount of CH_4 was produced which was gradually increased in Fe-loaded MMT/TiO_2 samples as depicted in Figure 4 (b). C_2H_6 production was not detected in the pure TiO_2 but its production was evidenced in MMT/TiO_2 and Fe-MMT/TiO_2 samples. The prominent C_2H_6 production in the presence of Fe was perhaps due to instant charge separation resulting in prolonged recombination time of the photo-generated charges (Harifi et al., 2014).

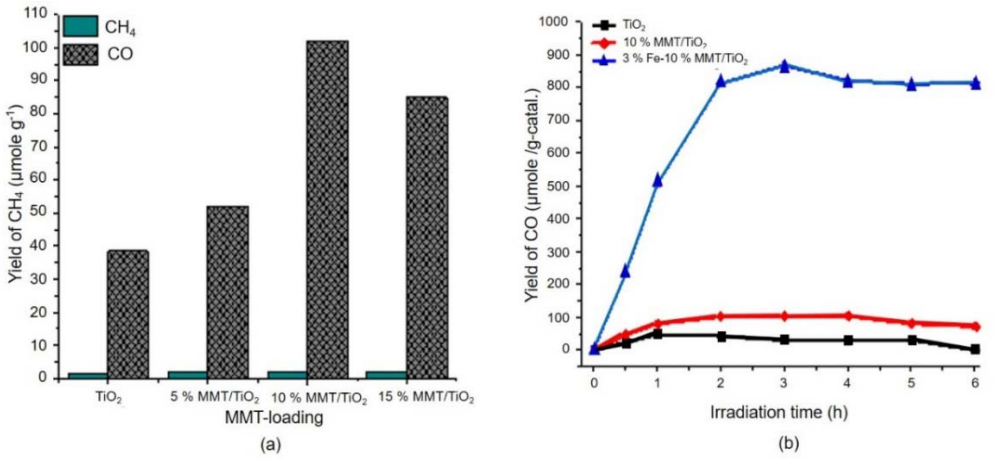

Figure 3: (a) Effect of MMT loading onto TiO_2 activity for CO_2 reduction with H_2; (b) dynamic CO evolution over Fe-TiO_2/MMT samples during at 100 °C, CO_2/H_2 ratio 1.0 and feed flow 20 mL/min

The yield rates of different products with their selectivity are presented in Table 1. The yield of CO over 3 % Fe-10 wt% MMT/TiO_2 was 289.30 µmole g-cat^{-1} h^{-1}, a 11.15 times more than the 10 wt% MMT/TiO_2 and 33.95 fold the amount produced over the pure TiO_2. The enhanced photoactivity was noticeably due hindered charges recombination rate by Fe and larger illuminated surface area in monolith microchannels (Tahir et al., 2016b). The selectivity for CO production over TiO_2 increased from 90.23 to 99.61 % in Fe-loaded TiO_2 samples. These results show that CO_2 can efficiently and continuously be converted to cleaner fuels using Fe-loaded MMT/TiO_2 catalyst and monolith photoreactor.

Table 1: Summary of yield rates and selectivity of products over TiO_2 and modified TiO_2 samples

Samples	Yield rate (µmole g-cat^{-1} h^{-1})			Selectivity (%)	
	CO	CH_4	C_2H_6	CO	CH_4
TiO_2	8.52	0.92	-	90.23	9.76
10 % MMT/TiO_2	25.95	0.53	0.06	97.91	2.02
3 % Fe - 10 % MMT/TiO_2	289.30	0.97	0.15	99.61	0.33

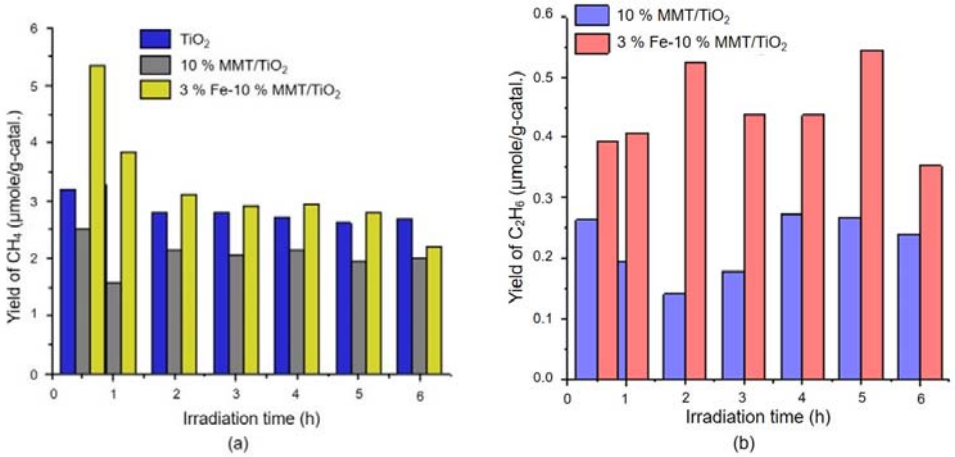

Figure 4: Effect of Fe-loading onto MMT/TiO_2 activity for CO_2 reduction with H_2; (a) CH_4 evolution; (b) CO evolution at 100 °C, CO_2/H_2 ratio 1.0 and feed flow 20 mL/min

During photocatalytic reveres water gas shift reaction, CO_2 is reacted with H_2 for the production of CO with smaller amounts of CH_4 and C_2H_6 as the potential products over MMT/TiO_2 samples. Possible reaction mechanism is illustrated in Eqs(1) to (5) (Tahir et al., 2013).

$$TiO_2 \longrightarrow e^- + h^+ \quad (1)$$

$$Fe^{2+} + 2e^- \longrightarrow Fe^{2+} - 2e^- \quad (2)$$

$$CO_2 + H_2 \longrightarrow CO + H_2O \quad (3)$$

$$CO_2 + 2H_2 \longrightarrow CH_4 + O_2 \quad (4)$$

$$2CO_2 + 3H_2 \longrightarrow C_2H_6 + 2O_2 \quad (5)$$

First, when the UV-light was irradiated to photocatalyst, electron-hole pairs were produced as explained in Eq(1). The photo-generated electrons can be trapped by Fe and metals in MMT, resulting in their efficient separation as explained in Eq(2). The electrons are transferred toward CO_2 for its reduction while holes are consumed for H_2 oxidation, resulting in reaction of CO_2 reduction (Eq(3)). The, H^+ radicals and active electrons can reduce CO_2 to CH_4 and C_2H_6 as explained in Eq(4) and (5). Figure 5 shows the reaction mechanism for photocatalytic CO_2 reduction with H_2 to fuels. As discussed previously, CO was the main product with selectivity above 99 %, confirming favorable CO_2 reduction process for production in a continuous flow monolith photoreactor and Fe-loaded MMT/TiO_2 photocatalysts. This significant amount of CO produced can be utilised in Fischer-tropschs for the production of cleaner fuels. Dynamic and selective CO production has confirmed that more CO_2 per unit time would be processed using continuous flow of photoreactor.

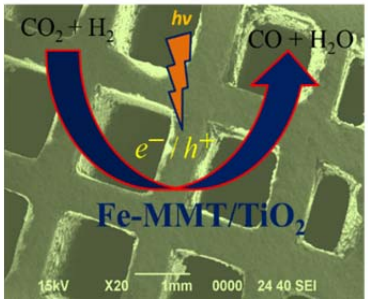

Figure 5: Schematic diagram of reaction mechanism for photocatalytic CO_2 reduction with H_2 to fuels

4. Conclusions

Photocatalytic CO_2 reduction with H_2 as a reducing agent for dynamic CO evolution over TiO_2 nanoparticles dispersed in MMT and loaded with Fe was investigated. The yield rate of CO_2 reduction was increased significantly by introducing Fe and MMT into TiO_2. The yield rate of CO as the key product observed over Fe-MMT/TiO_2 was 289.30 μmole g-cat^{-1} h^{-1} at selectivity 99.61 %, much higher when compared with pure MMT/TiO_2 and pure TiO_2 photocatalyst. The significantly enhanced photocatalytic activity was evidently due to hindered charges recombination rate by Fe and larger illuminated surface area in a monolith photoreactor. These results showed that Fe-loaded MMT/TiO_2 is an efficient photocatalyst for selective and dynamic photocatalytic CO_2 conversion to cleaner fuels.

Acknowledgement

The authors would like to extend their deepest appreciation to Universiti Teknologi Malaysia (UTM) and MOHE Malaysia for the financial support of this research under PAS-RUG (Potential Academic Staff Research University Grant, Vot 02k24) and FRGS (Fundamental Research Grant Scheme, Vote 02G826).

References

Bhattacharyya K.G., Gupta S.S., 2008, Influence of acid activation on adsorption of Ni(II) and Cu(II) on kaolinite and montmorillonite: Kinetic and thermodynamic study, Chem. Eng. J. 136 (1), 1-13.

Guo Q.S., Zhang Q.H., Wang H.Z., Liu Z.F., Zhao Z., 2016, Core-shell structured ZnO@Cu-Zn-Al layered double hydroxides with enhanced photocatalytic efficiency for CO_2 reduction, Catal. Commun. 77, 118-122.

Harifi T., Montazer M., 2014, Fe_3+:Ag/TiO_2 nanocomposite: Synthesis, characterization and photocatalytic activity under UV and visible light irradiation, Appl. Catal. A: Gen. 473, 104-115.

He Z.Q., Tang J.T., Shen J., Chen J.M., Song S., 2016, Enhancement of photocatalytic reduction of CO_2 to CH_4 over TiO_2 nanosheets by modifying with sulfuric acid, Appl. Surf. Sci. 364, 416-427.

Kameshima Y., Tamura Y., Nakajima A., Okada K., 2009, Preparation and properties of TiO_2/montmorillonite composites, Applied Clay Science 45 (1-2), 20-23.

Kočí K., Matějová L., Kozák O., Čapek L., Valeš V., Reli M., Praus P., Šafářová K., Kotarba A., Obalová L., 2014, ZnS/MMT nanocomposites: The effect of ZnS loading in MMT on the photocatalytic reduction of carbon dioxide, Appl. Catal. B: Environ. 158-159, 410-417.

Olivo A., Trevisan V., Ghedini E., Pinna F., Bianchi C.L., Naldoni A., Cruciani G., Signoretto M., 2015, CO_2 photoreduction with water: Catalyst and process investigation, J. CO2 Util. 12, 86-94.

Paulino P.N., Salim V.M.M., Resende N.S., 2016, Zn-Cu promoted TiO_2 photocatalyst for CO_2 reduction with H_2O under UV light, Appl. Catal. B: Environ. 185, 362-370.

Tahir B., Tahir M., Amin N.A.S., 2015a, Gold–indium modified TiO2 nanocatalysts for photocatalytic CO_2 reduction with H_2 as reductant in a monolith photoreactor, Appl. Surf. Sci. 338, 1-14.

Tahir B., Tahir M., Amin N.A.S., 2015b, Photoreactor Carbon Dioxide Reduction with Hydrogen in a Continuous Catalytic Monolith Photoreactor, Chem. Engin. Trans. 45, 259-264.

Tahir M., Amin N.A.S., 2013, Photocatalytic reduction of carbon dioxide with water vapors over montmorillonite modified TiO_2 nanocomposites, Appl. Catal. B: Environ. 142-143, 512-522.

Tahir M., Amin N.A.S., 2016a, Performance analysis of nanostructured NiO–In_2O3/TiO_2 catalyst for CO_2 photoreduction with H2 in a monolith photoreactor, Chem. Eng. J. 285, 635-649.

Tahir M., Tahir B., 2016b, Dynamic photocatalytic reduction of CO_2 to CO in a honeycomb monolith reactor loaded with Cu and N doped TiO_2 nanocatalysts, Appl. Surf. Sci. 377, 244-252.

Tahir M., Tahir B., Amin N.A.S., 2015c, Photocatalytic CO_2 reduction by CH_4 over montmorillonite modified TiO2 nanocomposites in a continuous monolith photoreactor, Mater. Res. Bull. 63, 13-23.

Yang M.Q., Xu Y.J., 2016, Photocatalytic conversion of CO_2 over graphene-based composites: current status and future perspective, Nanoscale Horiz. 1 (3), 185-200.

Yu W., Xu D., Peng T., 2015, Enhanced photocatalytic activity of g-C3N4 for selective CO_2 reduction to CH3OH via facile coupling of ZnO: a direct Z-scheme mechanism, J. Mater. Chem. A 3 (39), 19936-19947.